UNIVERSITY OF CALIFORNIA SAN DIEGO

Production and Analysis of Re-engineered Fusion Protein to Target Receptors on Cancer Stem Cells

A Thesis submitted in partial satisfaction of the requirements
for the degree Master of Science

in

Biology

by

Sanika Tikle

Committee in charge:

Professor Stephen Howell, Chair
Professor Dong-Er Zhang, Co-Chair
Professor James Kadonaga

2022

The Thesis of Sanika Tikle is approved, and it is acceptable in quality and form for publication on microfilm and electronically.

University of California San Diego

2022

TABLE OF CONTENTS

LIST OF FIGURES

ACKNOWLEDGEMENTS

I would like to acknowledge Dr. Stephen Howell, the chair of my committee and my MS Thesis advisor for the constant support and guidance.

I would also like to acknowledge all the lab members – Dr. Maria Mulero, Dr. Himangshu Sonowal, Dr. Xiying Shang, Clara Wong and Erika Barth – for their constant support and guidance.

ABSTRACT OF THE THESIS

Production and Analysis of Re-engineered Fusion Protein to Target Receptors on Cancer Stem Cells

by

Sanika Tikle

Master of Science in Biology

University of California San Diego, 2022

Professor Stephen Howell, Chair
Professor Dong-Er Zhang, Co-Chair

LGR5 and LGR6 receptors are present at high levels on the surface of epithelial stem cells of the ovary and Fallopian tube epithelia and the cancers that arise from these tissues (referred to as ovarian carcinomas). RSPO1 is a ligand for these receptors and, when bound, it drives WNT signaling and proliferation of cancer stem cells (CSC). Based on the hypothesis that RSPO1 could be used to target cytotoxic drugs selectively to CSC, the Howell lab developed a drug that contained 2 binding domains and armed this with the cytotoxin

monomethylaurostatin (R1FF-MMAE). Affinity of a ligand is a function of the number of binding sites and this thesis explored the question of whether the potency of R1FF-MMAE could be further enhanced by increasing the number of binding domains. A vector capable of expressing a protein containing 4 modified binding domains was constructed, and the FcST4-His protein was successfully produced in transiently transfected HEK293E cells and purified using nickel and ion exchange resins. Following arming with MMAE using the sortase reaction, this drug (FcST4-MMAE) was extensively characterized using gel electrophoresis, HPLC analysis on ion exchange and size exclusion columns, Western blot and cytotoxicity testing. The results disclosed that FcST4-MMAE could be purified to a grade sufficient for further development, and that it was remarkably stable at 4^{o}C and in the presence of a low pH of 3.0. However, cytotoxicity testing disclosed that the increase in binding domains did not enhance potency, perhaps due to the increase in size of the ligand and changes in the structure mediated by inter-domain interactions that interfered with access to the LGR5/LGR6 receptors.

INTRODUCTION

Ovarian cancer is the fifth leading cause of cancer deaths among women in the United States. With 95% of cases detected in the late stages, the 5-year survival rate for ovarian cancer patients is only 10% (Zhao, 2019). Most patients are diagnosed at an advanced stage ovarian cancer because the early-stage symptoms are non-specific and there is a lack of reliable early screening techniques (Stewart, 2019). With 314,000 women affected globally, 207,000 succumb to ovarian cancer every year making it the 6th most common cancer for women in the world (Globocan, 2020). Ovarian cancer is very heterogeneous and there are a variety of different molecular subtypes that make treatment challenging and survival rate low (Zhao, 2019). While patients often respond to chemotherapy initially, typically the disease recurs within months to a few years and 5-year survival in recent studies is only in the range of 40-50%.

As with other types of cancer, part of the problem is that, while chemotherapy can be quite effective at killing the more differentiated cells in the tumor, it is much less effective in killing the cancer stem cells (CSC) that support its proliferation. Stem cells are required to support the integrity of normal epithelia in the body such as the intestine and skin. Tumors also depend on primitive stem-like cells, referred to as CSC, that have many of the characteristics of the stem cells in normal tissues such as the ability to form spheroids and are responsible for the initiation of new metastatic sites (Batlle, 2017). In normal tissues stem cells proliferate in response to growth factors in their niche and their progeny gradually progress through a series of transcriptional states as they differentiate and lose proliferative potential (Songman Yu et al., 2021). Destruction of the stem cells results in loss of the epithelium. This concept appears to hold true also for many types of tumors. In principle, killing the very small fraction of cells in a

tumor that are CSCs should eliminate the supply of more differentiated tumor cells and stop tumor growth. Thus, developing drugs that can eliminate CSC is a major therapeutic goal (Clarke M., 2019)

CSCs as well as normal stem cells are regulated by WNT signaling which controls both proliferation and fate determination (Reya, 2005). Specifically, the R-spondin, family of four secreted proteins, interacts with leucine-rich coupled receptors, (LGR4, LGR5 and LGR6) to amplify WNT signaling which drives CSCs proliferation (Lebensohn, 2018). RSPOs block negative regulators of WNT signaling by neutralizing two transmembrane E3 ubiquitin ligases, ZNRF3 and RNF43 (Lebensohen, 2018), which in turn reduce the levels of WNT receptors on the cell surface. RSPO expression can be increased due to mutations in ZNRF3/RNF43 and this increase in expression can drive cancer. RSPOs contain furin-like repeats (Fu1 and Fu2) with through which they simultaneously bind LGR4-6 receptors through the Fu1 domain and the ubiquitin ligases ZNRF3/RNF43 through their Fu2 domain (Chen et al., 2013). The complex formation of RSPO with LGR4-6 and the ubiquitin ligases, triggers the clearance of ZNRF3/RNF43 (Peng et al., 2013) which results in the rise in WNT receptor levels on the cell surface. 2011). Ovarian cancer has one of the highest median expressions of RSPO1 mRNA which likely drives the growth and proliferation of its CSCs (Schindler, 2017). In addition, an analysis of data from the TCGA disclosed that high grade serous ovarian cancer (HGSOC) expresses uniquely high levels of the RSPO receptors LGR5 and LGR6; it has the highest level among all other tumor types with the exception of mesothelioma. Thus, ovarian cancer is a suitable target for exploration of the ability of RPSOs to direct cytotoxic drugs to CSC.

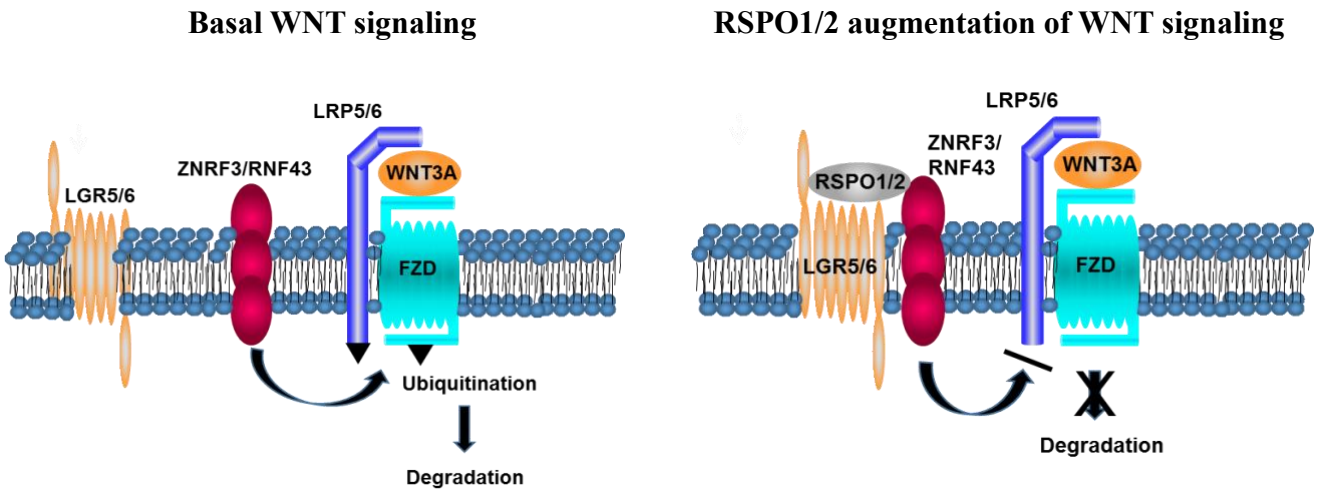

Figure 1. Reprinted from "LGR5 and LGR6 in stem cell biology and ovarian cancer" by S. Howell, 2017, Oncotarget.

Since abnormal activation of WNT pathway promotes CSC progression and leads to metastasis of cancer, major efforts are underway in the field to block WNT signaling with small molecules, antibodies, and antibody-drug conjugates (ADCs). Indeed, a very recent preclinical study from UCSD reported success with an ADC targeted to the FZD7 receptor (Do, 2020). However, thus far these approaches have had very limited success primarily due to off target effects. Due to the fact that the RSPOs bind to their receptors with very high affinities, another approach is to use an RSPO as a targeting moiety to carry a cytotoxin to CSCs. This approach may offer several advantages over antibodies that target LGRs for destruction of tumor stem cells. First, the penetration of ADCs is limited by their size. RSPOs are much smaller than an ADCs which favors deeper penetration and wider distribution within the tumor. Second, an RSPO has the potential to target all 3 of the LGR family members (LGR4, LGR5 and LGR6) at the same time whereas an ADC can target only a single LGR. Thus, an RSPO loaded with a cytotoxic warhead has the potential of killing cells that have a low expression of the targeted LGR but substantial expression of one of the other family members. Overall, this is expected to result in the death of a larger fraction of stem-like cells in a tumor. Third, the fact that RSPOs

simultaneously engage both an LGR and one of its co-receptors (ZNRF3 or RNF43) may enhance the rate and extent of internalization. Fourth, given the difference in size and physical characteristics, RSPOs may traffic with greater efficiency to the lysosome where the MMAE is released. Since the RSPO receptors LGR4, LGR5, and LGR6 are expressed only in stem cells, this strategy offers a level of selectivity not attainable with antibodies to the FZD receptors. Overall, there is a strong rationale for the further development of drugs based on the use of one or another RSPO.

One of the challenges in using antibodies or any other type of protein to target cytotoxic drugs to cancer cells is control of where the cytotoxin gets linked and how many cytotoxin molecules get loaded per molecule. Specifically for the drug conjugate we were working on, a single molecule of MMAE was conjugated to the C-terminal end of the Fu1-Fu2 domain using the sortase reaction. The sortase reaction was chosen because of the high reaction efficiency and the stability of the val-cit-PAB linker in the systemic circulation. Moreover, sortase mediated reactions are site specific and the reaction time can be optimized for higher final product yields. As shown in the figure below, the target protein is engineered with a sortase recognition sequence (LPETGG) on the C terminal end. The enzyme sortase recognizes this sequence and cleaves after the threonine in the LPETGG sequence removing the GG-8xHis fragment and substituting the GGG-vc-PAB-MMAE. The ratio of the protein to the cytotoxin was optimized such that the forward reaction is favored to yield the final product R1FF-MMAE.

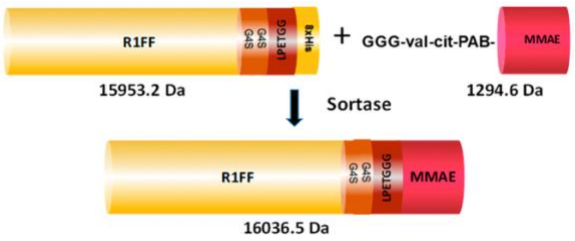

Figure 2. Reprinted from "Therapeutic Targeting of Tumor Cells Rich in LGR Stem Cell Receptors" by Songman Yu, 2021, Bioconjugate Chemistry.

The Howell lab began exploring the use of RPSOs as targeting moieties several years ago. The work started with RPSO1 and, rather than using the full-length molecule that includes 2 furin-like domains, a thrombospondin domain, and a C-terminal basic domain, they chose to use just the furin domains that contain the LGR binding sequences. The sortase reaction was chosen as the tool for loading the very potent tubulin inhibitor monomethylauristan E onto the protein. The resulting molecule, R1FF-MMAE, was shown to have nanomolar potency against ovarian cancer cell lines i*n vitro*, a favorable terminal plasma half-life in mice and anti-tumor activity in 3 human ovarian cancer xenograft models (Yu, 2021). However, it turned out that this protein was difficult to produce in transiently transfected HEK293 or ExpiCHO systems and tended to aggregate during purification. Thus, not enough of the precursor protein could be made to advance the molecule into pre-IND studies. The challenge presented to me was to identify other approaches to using RPSOs as targeting moieties, build the molecules, characterize their pharmacologic characteristics, and then assess their efficacy.

RESULTS

CHAPTER 1: PRODUCTION, PURIFICATION AND CHARACTERIZATION OF FcST4-MMAE

In approaching this project, I took into consideration that different RSPOs varying in their binding affinities to LGR4, LGR5 and LGR6, that it would be advantageous to have a higher affinity than what was attained with R1FF-MMAE, and that longer initial and terminal half- lives may result in better tumor accumulation. One way to increase avidity is to increase the number of binding sites in a molecule (Erlendsson, 2021). R1FF-MAME contained one copy of the Fu1-Fu2 domain that mediates binding to the LGRs. Increasing this to 2 or even 4 copies had the potential of increasing avidity to a large degree. A commonly used strategy for increasing plasma half-life is to add an immunoglobulin Fc domain to the molecule. The Fc domain binds to FnRc receptors in the liver which, rather than allowing IgG molecules that are captured by the liver to be broken down, recycles them to the cell surface where they are released back into the circulation. Given these considerations, I changed around the components and designed a new molecule, FcST4, that contains a proprietary Fc domain, components of 4 LGR-binding domains, and the sortase recognition sequence followed by an 8x His tag (LPETGG-HHHHHHHH) at the C-terminal end.

1.1 Construction of the FcST4-His vector

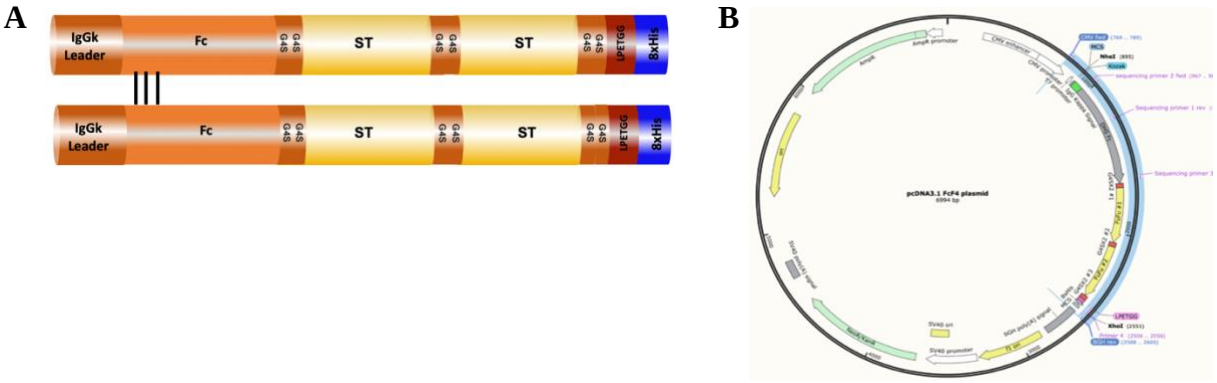

Figure 3. Vector construction of FcST4. A. Steps to obtain the FcST4 DNA construct by overlapping two fragments **B.** Schematic diagram of the FcST4 pcDNA3.1 vector.

A vector construct for the FcST4 molecule was designed to contain an IgG leader sequence on the N terminal end, followed by a mutated Fc domain attached to two modified receptor binding domains (ST) in series with a linker sequence in between the two ST domains. A second spacer sequence was inserted just upstream of the LPETGG sortase recognition (donor) motif and an 8xHis tag was positioned at the C terminal end. Figure 1A shows the schematic of the steps used to create the FcST4 vector employing an overlap PCR technique. Restriction enzyme double digestion was used to two create two DNA fragments from an existing FcST2 vector such that both fragments had an overlap in the linker sequence in common that would allow annealing of the two fragments. Appropriate primers were designed to amplify both fragments separately first, and then the two fragments were annealed at 70^{o}C to generate a final product. The final product was ligated to pcDNA3.1 as shown in Figure 1B. Sanger sequencing of a maxiprep was used to confirm that the sequence was 100% match to the planned sequence, and subsequently the ligated vector was stored at -80^{o}C to use for transfection.

1.2 Production an initial purification and characterization of FcST4-His in HEK293E

The full-length protein was produced in HEK293E cells. The FcST4.pcDNA3.1 vector was transiently transfected in HEK293E cells. The HEK293E cells were allowed to grow in Freestyle 293 media for 5 days before being used for transfection. On the day of transfection, the cell media was refreshed and a mix containing the FcST4.pcDNA31 vector and PEI 25K (1 mg/mL) was added dropwise to the 150 mL transfection flask and incubated at 130 rpm, 5% CO2, for 4 hours. Four hours after transfection, the flask was supplemented with 150 mL of HySFM293 media and 30 mL of Freestyle 293 media to bring the final volume upto 300 mL. The cells were allowed to grow. Approximately 24 hours after transection, valproic acid and 1:1000 v/v anti-clumping agent was added to the flask containing transfected HEK293E cells. The cells were harvested on day 5. The mean cell viability on the day of harvest for the 7 batches of FcST4 produced was 79%.

After harvest, the cell supernate was processed through the initial steps of purification. The first purification step was based on the ability of the 8xHis tag to bind to Ni resin. Particulate manner was removed by high-speed centrifugation of the cell supernates and then loaded on gravity flow column packed with pre-charged Ni-NTA resin. The FcST4-His was eluted using 300 mM imidazole and the protein was then passed through a DEAE column and the flow-through was characterized using HPLC reverse-phase C4 column and non-reducing SDS/PAGE gel analysis.

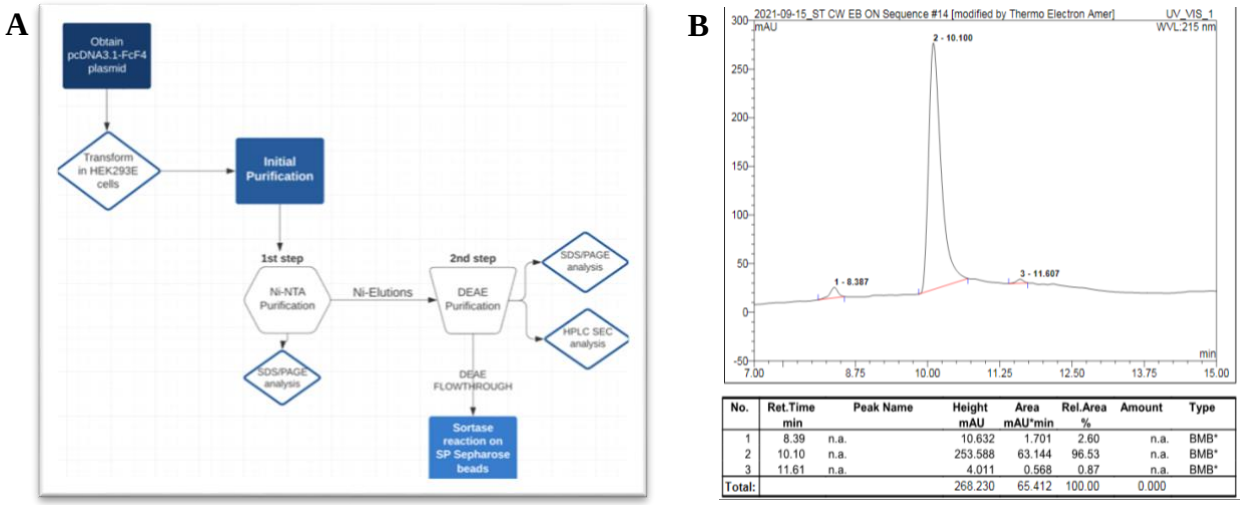

No.	Ret.Time min	Peak Name	Height mAU	Area mAU*min	Rel.Area %	Amount	Type
1	8.39	n.a.	10.632	1.701	2.60	n.a.	BMB*
2	10.10	n.a.	253.588	63.144	96.53	n.a.	BMB*
3	11.61	n.a.	4.011	0.568	0.87	n.a.	BMB*
Total:			268.230	65.412	100.00	0.000	

Figure 4. Initial Purification Scheme and HPLC-C4 analysis of FcST4-His. A. Schematic of the production and purification process of FcST4-His. **B.** HPLC-C4 trace of FcST4-His after 2nd step DEAE purification.

The presence of the Fc domain on the N-terminal end of the protein is expected to dimerize the 2 ST2-His chains resulting in a protein whose MW calculates to be 114 kD but, because of glycosylation may run at a higher MW. The HPLC C4 analysis showed a sharp peak at 11.89 min corresponding to FcST4-His (Fig. 4B) consistent with a protein of approximately 120 kD. The tiny peak at 8.3 minutes may be an FcST4-His monomer; the very small peak at 11.6 min was not further characterized. The SDS-PAGE analysis disclosed the presence of 3 bands migrating at 112, 224 and 336 kD (Fig. 4B). The 224 kD band is consistent with the expected size of a tetramer (i.e., a dimer of the already Fc-dimerized protein) and the highest band with that of an octamer. The protein was remarkably pure even after just these first two steps of purification.

1.3 Exploration of initial purification strategies for FcST4-His (Ni, DEAE)

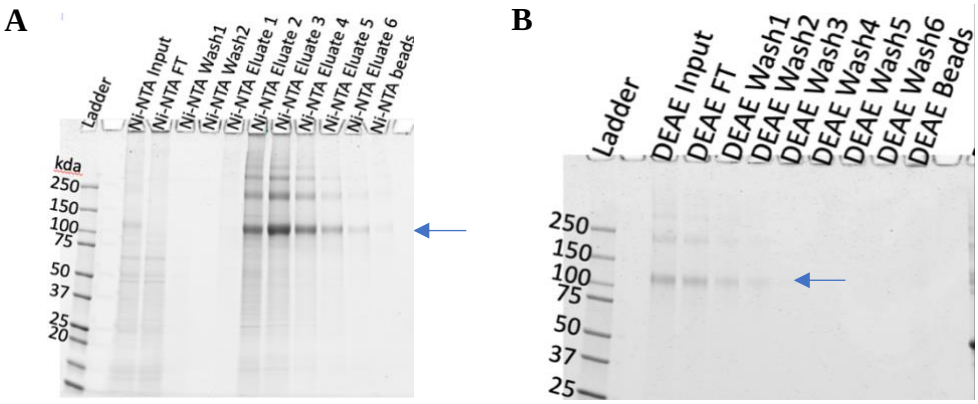

Figure 5. SDS-PAGE analysis of fractions collected from the Ni and DEAE columns. **A.** Non-reducing SDS/PAGE gel showing successful elution of the FcST4-His indicated with a correct sized dimer band marked with blue arrow. **B.** Non-reducing SDS/PAGE gel showing a pure final FcST4-His protein with a correct sized dimer band indicated with a blue arrow.

The results of the initial Ni purification step were examined in more detail by collecting and analyzing fractions from serial wash and elution steps with 300 mM imidazole, and the sequential flow-through and wash steps of the DEAE column (Figure 5A & B). The ratio of band sizes did not vary with serial elutions indicating no selective purification of the 120 kD FcST4-His dimer could be achieved with this strategy. The DEAE step was successful in removing some of the HMW forms; an average of 28% of the FcST4-His was lost in this step. However, this loss was mostly the result of successful retention of HMW forms on the DEAE resin. Use of the serial Ni-NTA and the DEAE steps resulted in a reasonably pure form of FcST4 that then served as the input to the sortase reaction that conjugated the MMAE onto the molecule. The first step Ni-NTA purification and the second step DEAE purification resulted in a reasonably pure FcST4-His protein as evident by the presence of a single peak in the HPLC-C4 profile (Fig 4B).

1.4 Exploration of Protein A as a purification strategy for FcST4-His

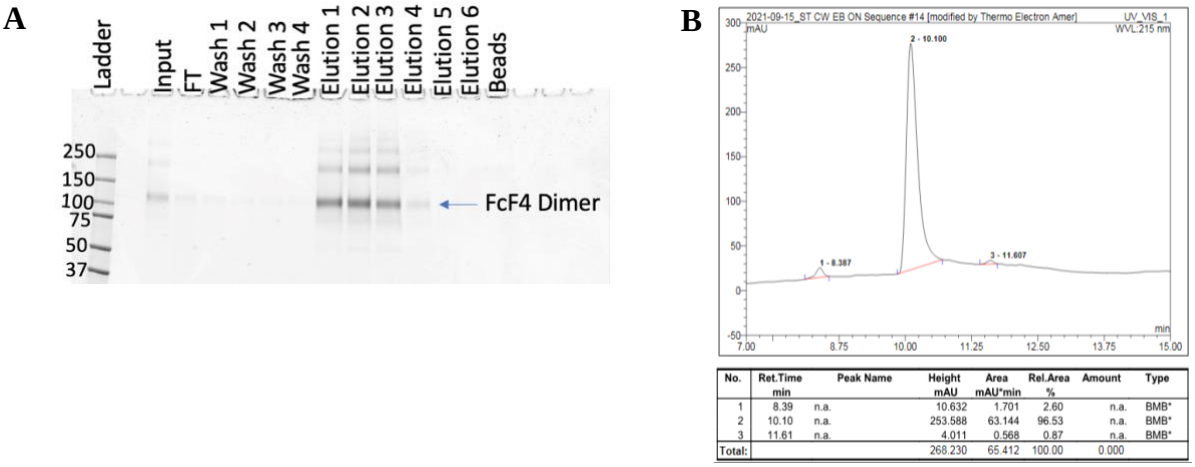

Figure 6. Analysis of FcST4-His after Protein A purification using HPLC and SDS/PAGE gel. A. Non-reducing SDS/PAGE analysis of eluted fractions. **B.** HPLC-C4 analysis of combined Protein A eluates.

Though the Ni-NTA and DEAE purification methods produced a quite pure FcST4-His protein, an additional purification strategy was explored using the Protein A resin in order to take advantage of the presence of an Fc domain in the FcF4 structure which binds very tightly to Protein A. Figure 6A shows that the protein was successfully captured from the cell supernate by the Protein A resin, and that it was successfully eluted with PBS containing 1 M NaCl as evidenced by a correct sized band on the SDS/PAGE gel. However, only 66% of the protein could be eluted off the Protein A resin. The remaining 46% either remained bound to the resin beads or was found in the flow through and the washes as seen in Figure 6A.

The eluates from the Protein A purification were combined and analyzed using the C4 reverse-phase HPLC column. Figure 6B shows a single peak at the correct elution time of 10.1 minutes, but the trace also shows the presence of tiny peaks around 7 min and 11 min. Considering that the HPLC-C4 trace of FcST4-His was not as clean as the trace achieved after

the DEAE purification (Figure 4B), the use of Protein A resin for purification was not explored further.

1.5 Coupling of MMAE to FcST4-His using the Sortase Reaction

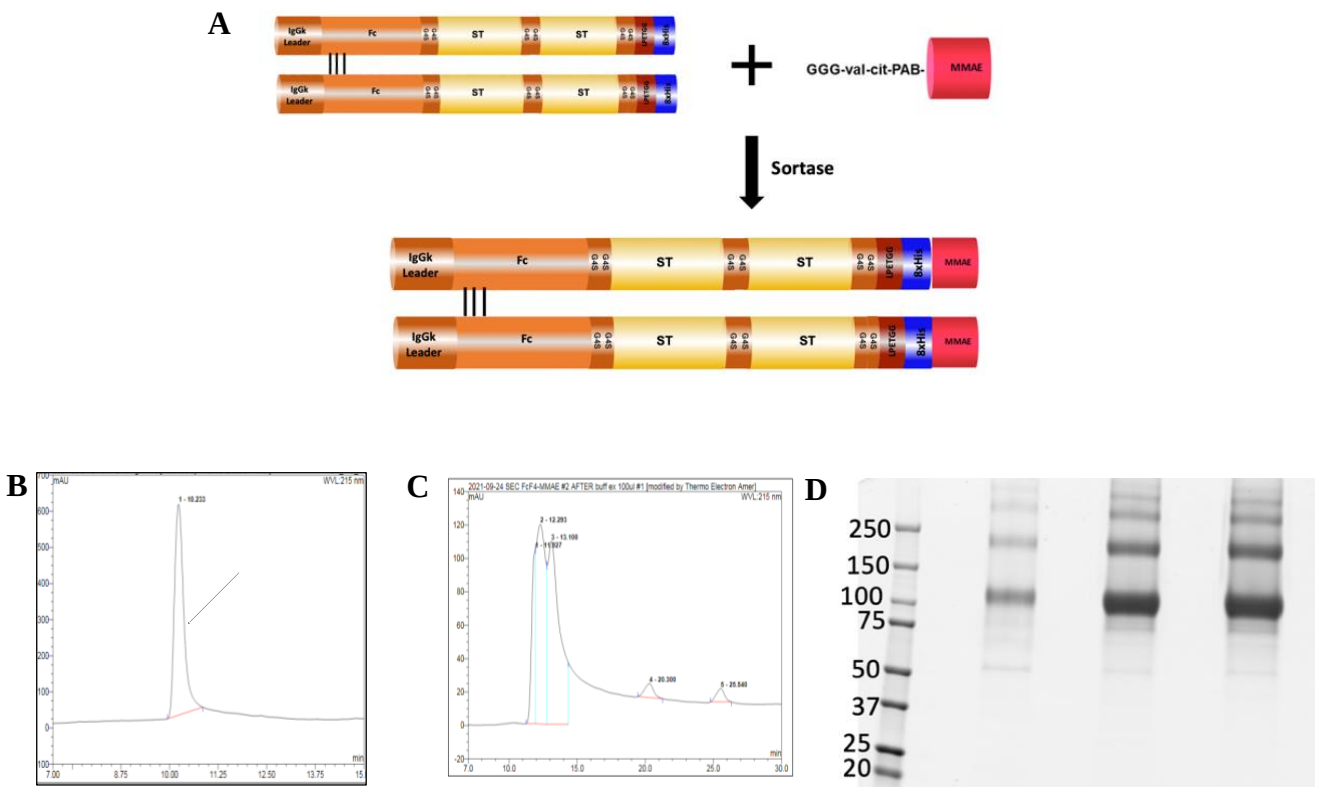

Figure 7. HPLC Profiles of the Final FcST4-MMAE Product Showing the Purity of the Sample. A. Schematic diagram of the synthesis of FcST4-MMAE. G3-MMAE is coupled with FcF4 using a sortase reaction. **B.** Documentation of the purity of FcST4-MMAE using the HPLC-C4. **C.** HPLC-SEC150 profile of final product. **D.** Non-reducing SDS/PAGE of the first 3 batches of FcST4-MMAE. The black arrow shows the FcST4-MMAE dimer, and the blue arrow shows the tetramer.

Following the Ni-NTA and DEAE purification, the FcST4-His was linked to the cytotoxin monomethylaurostatin (MMAE) using a sortase reaction. The sortase enzyme cuts between the threonine and the glycine in the LPETGG tag removing the GG-8xHis tag. The sortase reaction was carried out with the precursor FcST4-His loaded on the cation exchange

resin SP-sepharose. This allowed the excess G3-val-cit-PAB-MMAE and sortase enzyme to be washed away prior to elution of the SP-sepharose with 1 M NaCl. The efficiency of the sortase reaction across all batches of FcST4-His was 100 ± 37 % (SD). However, the average percent yield of the final product was 90 ± 22% (SD) post sortase reaction.

The elution time of the FcST4-MMAE was approximately 1 min later than that for the FcST4-His on the HPLC-C4, such that FcST4-His was eluted at 10.1 min and FcST4-MMAE at 10.2 minutes (Figure 7B). This was used as a measure to confirm that the sortase reaction had been completed successfully. The purity of the final product was documented using the HPLC-C4, HPLC-SEC130 and an SDS/PAGE gel analysis. A single peak observed in the HPLC-C4, and the HPLC-SEC traces confirmed the purity of the final product FcST4-MMAE (Figures 7B and C).

The band patterns of the final product were also confirmed using non-reducing SDS/PAGE gel analysis as shown in Figure 7D for the first three batches of FcF2-MMAE. The bands correspond to the FcST4-MMAE dimer, tetramer, and an additional high molecular form of the protein.

1.6 Yield During Production of Serial Batches

Table 1. Yield of all the batches of FcST4-MMAE produced.

FcST4-MMAE Batch Number	**1**	**2**	**3**	**6**	**7**
Amount of Final product per Liter of culture (mg/L)	14.94	12.99	8.33	6.91	15.8
Overall Percent Yield (%)	100	100	80	98	76

Once a workflow for the purification strategy followed by the sortase reaction was devised, subsequent batches were produced using an identical workflow. The amount of final product

obtained per liter of culture varied across cultures as shown in Table 1. The percent yield was calculated by comparing the milligrams of FcST4-His protein obtained after the DEAE purification versus the amount obtained after the completion of the sortase reaction, and the average yield was 90 ± 22% (SD).

1.7 Stability of FcST4-MMAE with Increasing Amounts of Freeze/Thaw Cycles

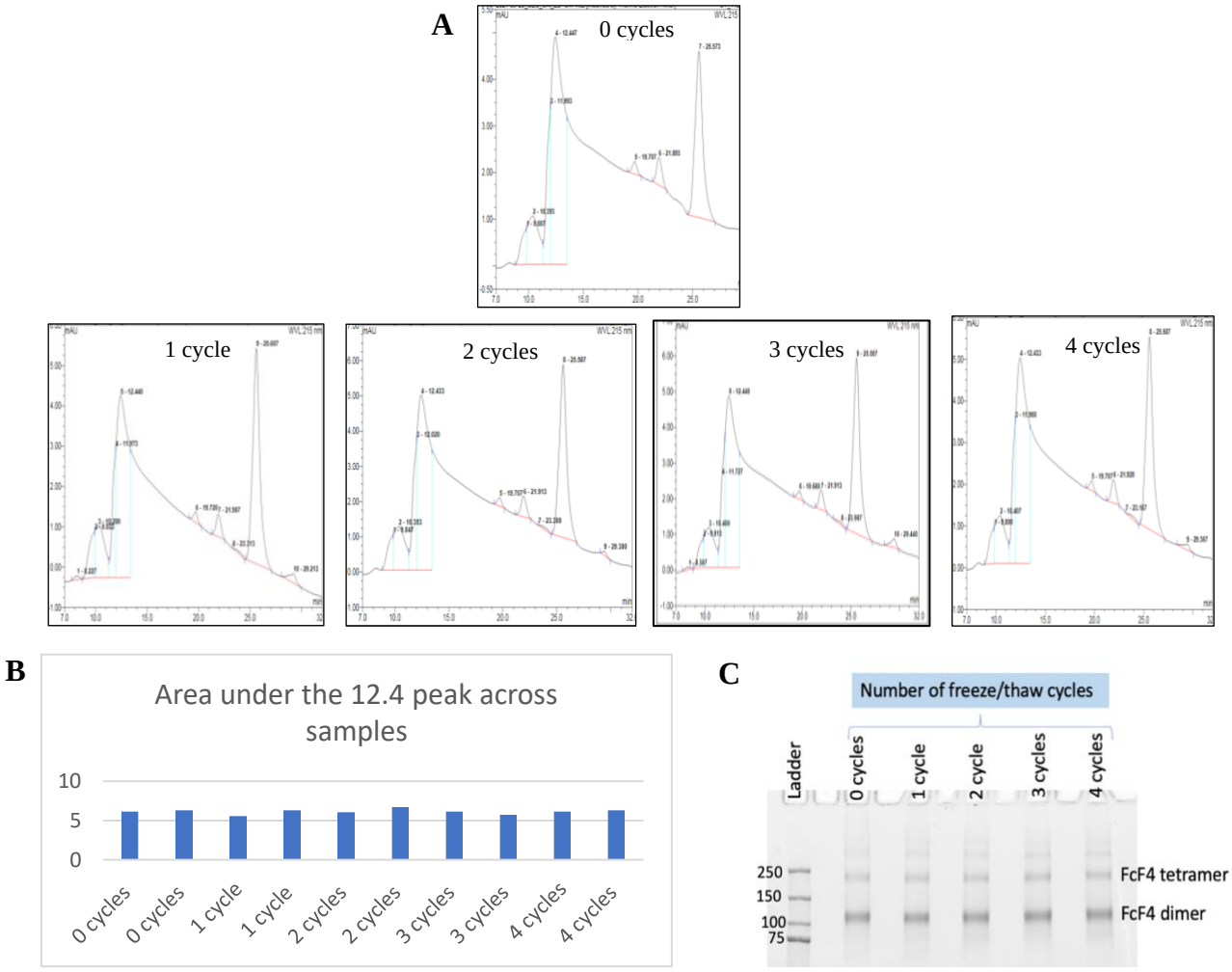

Figure 8. HPLC and SDS/PAGE Analysis of the Effect of Freezing and Thawing on FcST4-MMAE. A. Documentation of the change in the HPLC-SEC trace of FcST4-MMAE with increasing freeze/thaw cycles. **B.** Histogram of the area under the main 12.4-min peak of FcST4-MMAE before and after each freeze/thaw cycle. **C.** Non-reducing SDS/PAGE gel analysis of the change in FcF2-MMAE bands with increasing numbers of freeze/thaw cycles.

To assess the stability of the FcST4-MMAE molecule, the sample was subjected to multiple freeze and thaw cycles. Figure 8A shows that there was no significant change in the SEC130 trace of the FcST4-MMAE molecule even after 4 cycles. There is consistency in the number of peaks seen across profiles. Additionally, the area under the main peak of FcST4-MMAE at 12.4 min did not change with increasing cycles of freeze/thaw (Figure 8B). More

importantly, the non-reducing SDS/PAGE gel in Figure 8C strengthens the evidence that there is no change in the structure of FcST4-MMAE as there is consistency between the bands observed in all samples on the gel. This experiment showed that FcST4-MMAE is a very stable with respect to freezing and thawing and can be subjected to at least 4 cycles without it affecting the structure of the protein as detected by SEC130 and SDS/PAGE analysis.

1.8 Stability of FcST4-MMAE at 4ºC and 37ºC

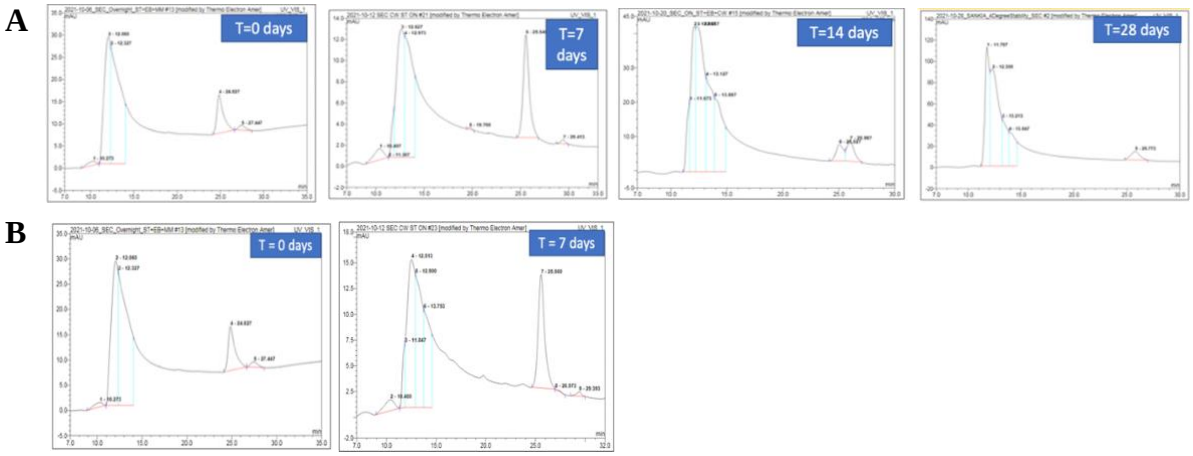

Figure 9. HPLC-SEC130 profiles documenting change in the FcST4-MMAE over 7 d at 4ºC or 7 d at 37ºC. A. HPLC-SEC130 traces of FcST4-MMAE at different time points over a period of 28day incubation at 4oC. **B.** HPLC-SEC traces of FcST4-MMAE at different time points over a period of 7-day incubation at 37oC.

After assessing the stability of FcST4-MMAE during multiple freeze/thaw cycles, the stability was determined at 4ºC and 37ºC by analyzing change in the SEC130 profile at different time points. Figure 9A shows that storing the FcST4-MMAE at 4ºC causes minor changes in the SEC130 trace. After 14 days of storage at 4ºC, the 12.4 min peaks start developing a shoulder while at the end of 28 days that same shoulder turns into another sharp peak with tiny shoulders next to it. This shows that storage at 4ºC for long periods of time can affect the size distribution of the protein. Figure 9B shows that storage for 1 week at 37ºC significantly affected the

SEC130 trace of FcST4-MMAE. The peak eluted at 12.5 min started to develop a shoulder and the peak eluted at 25 min increased 3 times in area. Overall, this stability assay demonstrated that storage at either 4°C or 37°C is not ideal as documented by the changes in size distribution.

1.9 SEC Analysis and Characterization of Fractions

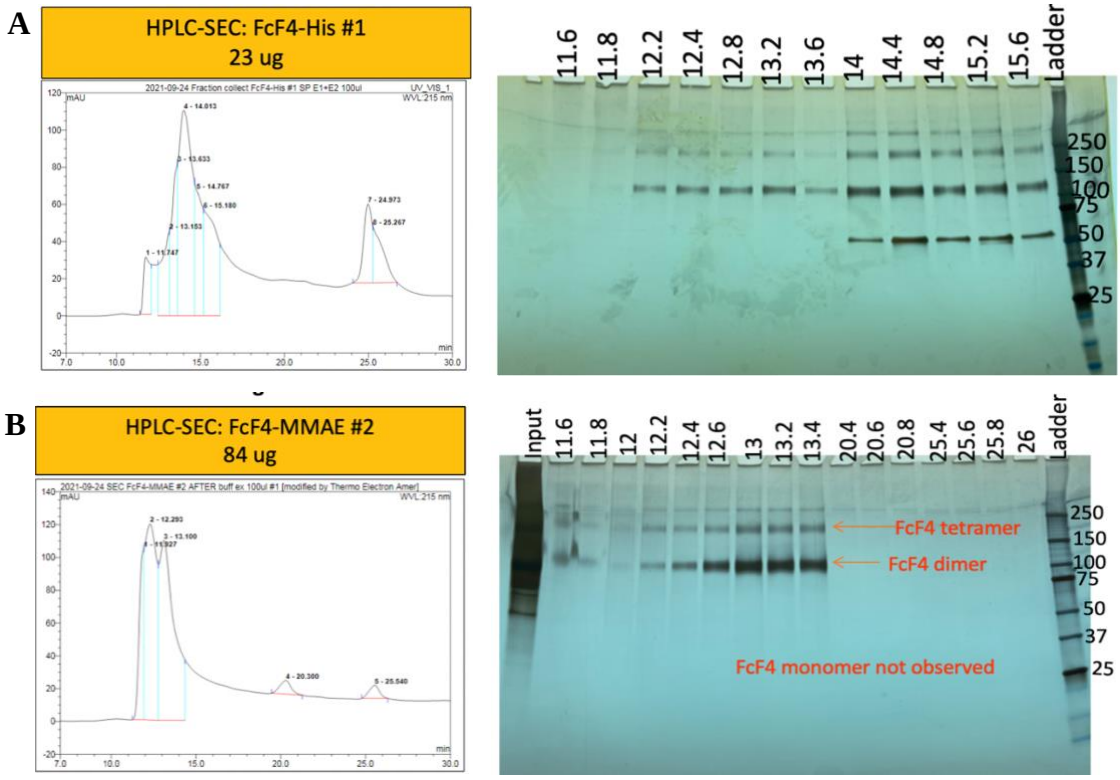

Figure 10. SEC130 and SDS/PAGE Analysis of the FcST4-His and the FcST4-MMAE Fractions Collected from the HPLC-SEC130. A. HPLC-SEC130 trace of FcST4-His with a non-reducing SDS/PAGE analysis of the fractions collected from the HPLC column. **B.** HPLC-SEC130 trace of FcST4-MMAE with a non-reducing SDS/PAGE analysis of the fractions collected from the HPLC column.

To understand which molecular weight form of FcST4-His and FcST4-MMAE is represented by the peaks on the SEC130 column, fractions were collected from the major peaks for each and analyzed by non-reducing SDS/PAGE gel. This resulted in a clear indication of the forms of the proteins. However, the SEC analysis really did not help much; it was impossible to

assign any one peak to a particular MW because all peaks contain a fair amount of each one of the forms. Thus, except perhaps for indicating the presence of very low MW forms, the SEC130 cannot be used to assess the quality of each batch of protein.

1.10 Cytotoxicity of FcST4-MMAE in HEK293/EV vs HEK293/LGR5 in comparison to FcST4-MMAE

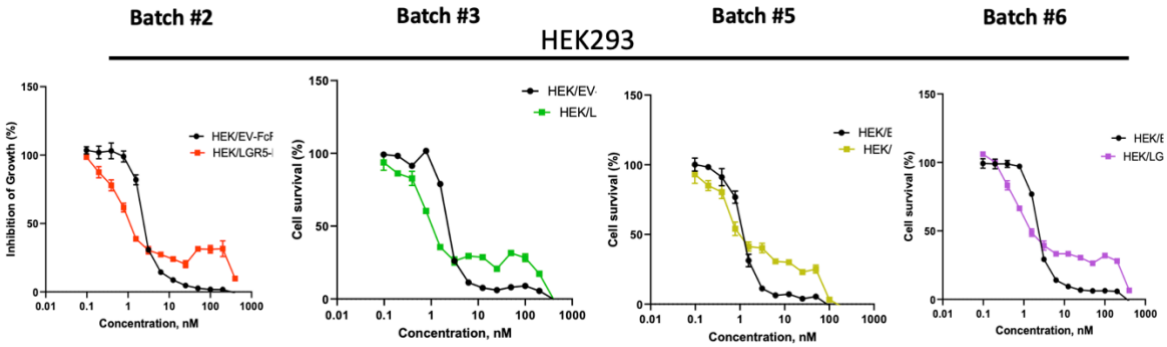

Figure 11. Cytotoxicity Assay of FcST4-MMAE Batches in HEK293T Cells.

After the production of 7 batches of FcST4-MMAE, batches 2-6 were used to do a cytotoxicity assay by another member in the lab. The HEK293 cells were grow and treated with the drug in a 96-well plate in a series of concentrations starting from 0 mM to 400 mM. On day 6, CCK8 reagent was added and the OD450 of the experimental plates was read.

Consistently for FcST4-MMAE batches 2-6, Figure 11 shows that eventhough there is a difference in targeted killing in HEK293 empty vector cells versus cells overexpressing LGR5 receptors, the different isn't significant.

1.11 Cytotoxicity of FcST4-MMAE in OVCAR8/EV vs OVCAR8/LGR5 in comparison to FcF2-MMAE

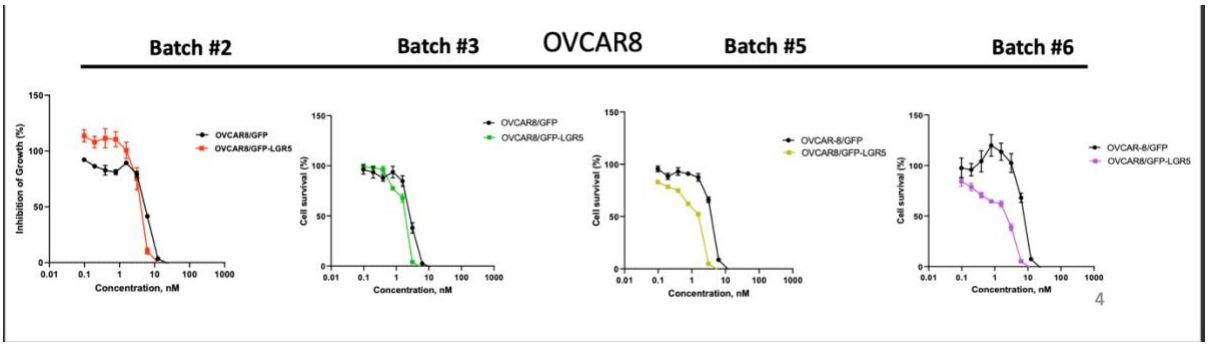

Figure 12. Cytotoxicity Assay of FcST4-MMAE in OVCAR8/EV and OVCAR8/LGR5 Cells.

The cytotoxicity assay was for FcST4-MMAE was also done using the OVCAR8 cell line. Concentration of the drug starting from 400 nM to 0 mM was tested.

Similar to the results observed in Figure 11 with the HEK293e cells, eventhough there was some amount of difference in targeted killing between OVCAR8 cells expressing just the empty vector and cells engineered to overexpress LGR5 receptors, the difference wasn't significant. The IC_{50} values ranged from 1.9 to 3.8 nM

1.12. Summary of Conclusions for FcST4-MMAE

A series of experiments done to assess the purity, yield, and potency of the FcST4-MMAE molecule revealed that though the molecule is relatively stable when stored over time, it failed to show differential killing between the empty vector cells and cells overexpressing LGR5 receptors in two different cancer cell lines. Additionally, with production of the multiple batches of FcST4-MMAE it became increasingly clear that the low yield of 14 mg/L culture could not be further improved. Therefore, subsequent work was focused on assessing the stability and cytotoxic properties of the FcST22-MMAE molecule.

CHAPTER 2: ANALYTICAL STUDIES OF FCST2-MMAE

There are several reasons why the FcST4-MMAE molecule failed to demonstrate the same or greater degree of selective cytotoxicity as was originally observed with the R1FF-MMAE molecule. Addition of the Fc domain, changes made in the receptor binding domains, the overall change in size and number of glycosylation sites may all have played a role. To try to retain the benefit of having an Fc domain to both act as a chaperone during folding and to confer a longer plasma half-life, the FcFST4-His molecule was redesigned such that it contained only one ST domains rather than two in each arm of the molecule as shown in Figure 5A. The vector for expression of this protein as designed and build by one of the other members of the Howell lab. I took over work on the molecule after it was first established that it could be expressed in the transient transfection HEK293 system.

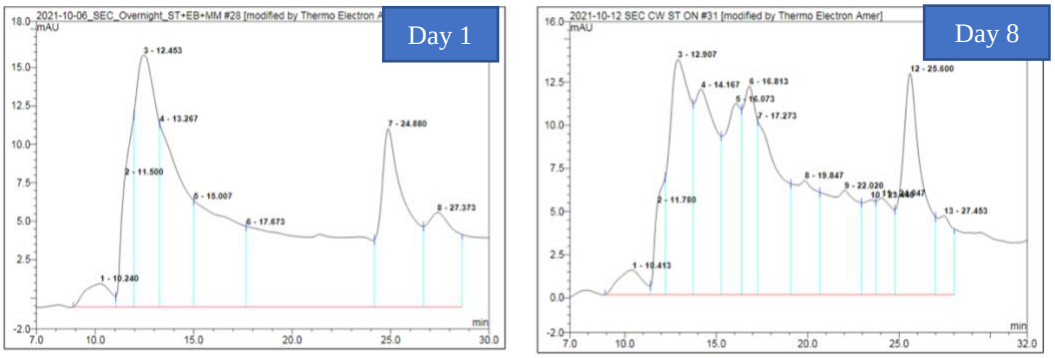

Figure 13. HPLC SEC130 trace of FcST2-MMAE after 7-day incubation at 37ºC

A study done by another Howell lab member showed that when incubated at 37ºC for 1 week, the shape of the HPLC SEC130 trace of the FcST2-MMAE protein changed significantly. More peaks became apparent and the area of the peaks eluting at 16.1 to 17.3 min increased (Figure 13). This experiment demonstrated a clear shift in the size distribution of freshly made

FcF2-MMAE after 1 weeks of storage at 37ºC. These changes observed emphasized the need to explore the role of excipients in stabilizing the protein and preventing shifts in the SEC traces.

2.1 Effect of Excipients on the Stability of FcST2-MMAE

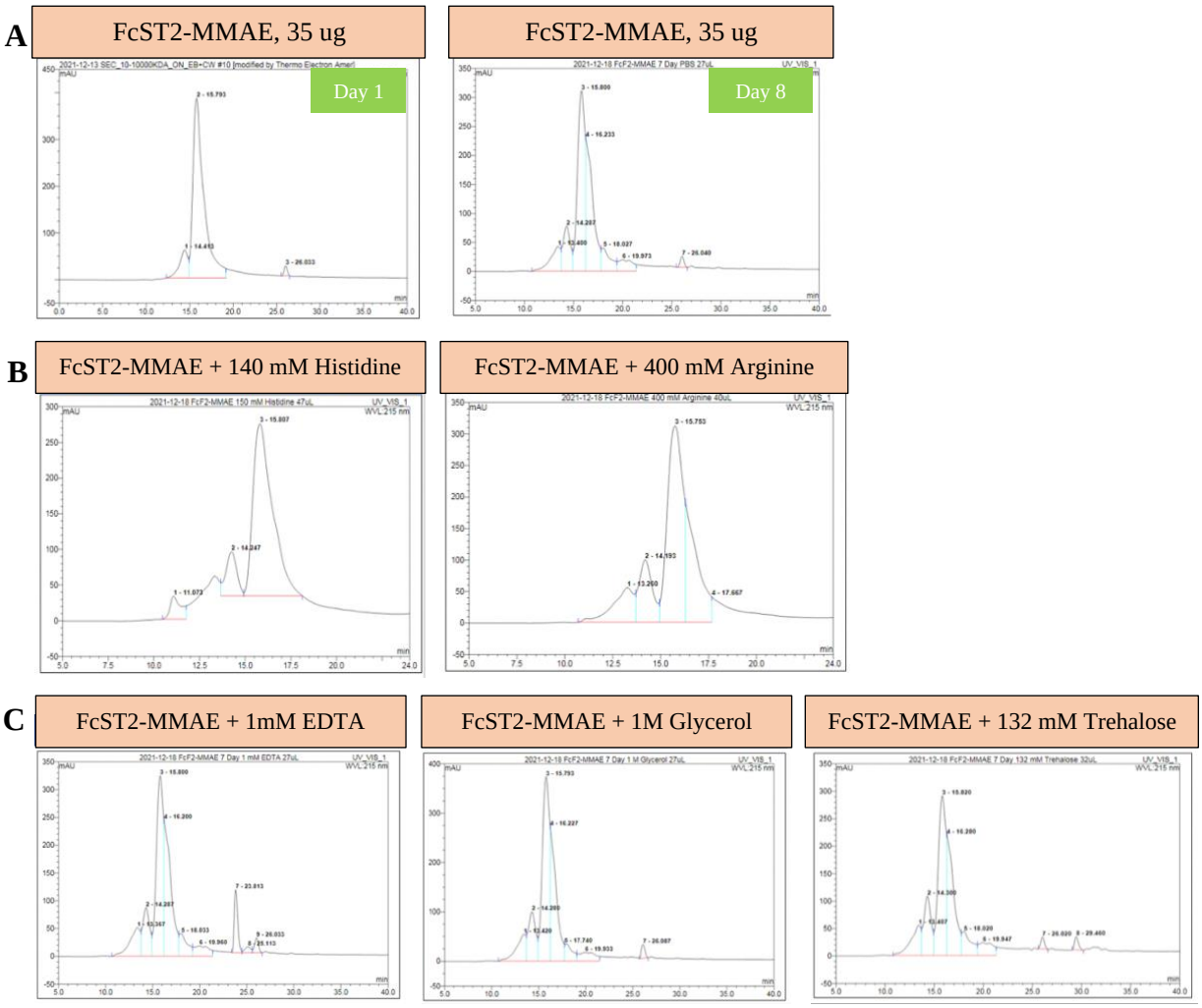

Figure 14. Analysis of the Effect of glycerol, EDTA and trehalose on the Stability of FcST2-MMAE using HPLC-SEC300. A. HPLC-SEC300 trace demonstrating the change in the FcST2-MMAE profile after 1 week of storage at 25ºC. **B.** HPLC-SEC300 trace showing the immediate change caused in the FcF2-MMAE profile after addition of 150 mM histidine and 400 mM arginine. **C.** HPLC-SEC300 showing the effect of glycerol, EDTA and trehalose in stabilizing the FcST2-MMAE.

Given the changes in FcST2-MMAE that occurred at 37ºC, a literature review was conducted to identify excipients known to stabilize proteins in solution and arginine, histidine, trehalose,

glycerol and EDTA were identified as candidates to be tested. The concentrations selected for testing correspond to those most commonly found in commercial formulations of protein drugs. Each excipient was injected alone in the HPLC-SEC300, and the peaks representative of each excipient also appeared when mixed with the FcST2-MMAE protein.

Figure 14 shows that, in the absence of added excipients, FcST2-MMAE incubated at 37°C for 7 days (Day 1 – Day 8), the protein underwent multiple changes with the appearance of 4 new peaks and a reduction in the 15.8 min peak from 86 to 69% of the total AUC. Addition of 400 mM arginine caused the immediate appearance of a peak at 13.26 min which corresponds to a MW of 463 kD. This is very similar to the 13.4 peak (494 kD) that was observed in the PBS only sample on Day 8. Addition of 150 mM histidine caused immediate appearance of two new peaks, one at 11.07 min (1138 kD) and another at 13.4 min (463 kD); the latter is the same as seen when arginine was added and, in the PBS, only sample on Day 8. At the concentrations tested, neither glycerol, EDTA or trehalose provided any detectible stabilizing effect (Figure 14 C). On Day 8 there are no significant differences in percent of AUC in each peak for these 3 excipients relative to the sample for PBS alone. Arginine and histidine generated a small amount of higher MW species similar to what is seen in the PBS sample on Day 8.

2.2 Testing the Concept that Low pH Might Precipitate HMW forms

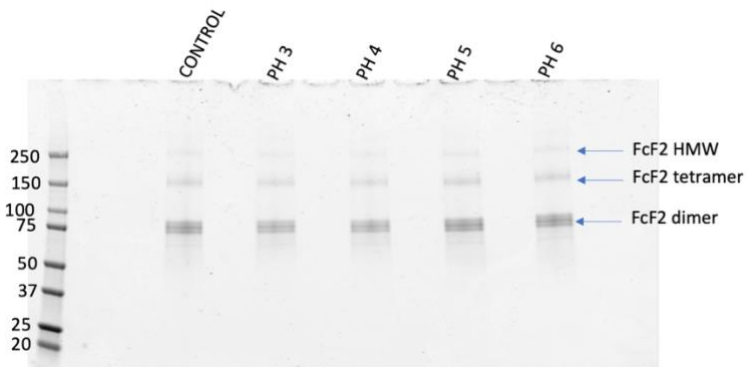

Figure 15. Non-reducing SDS/PAGE Analysis of Samples Incubated with Citrate Buffer at pH 3.0, 4.0, 5.0 and 6.0

Both the SDS/PAGE and SEC300 indicated the presence of higher molecular weight (HMW) forms of the protein in the purified FcST2-MMAE product. Aggregates and multimers of some other proteins with structural similarities to RSPO1 are known to differentially precipitate inn low pH buffers, and this has been used to enhance the purity of the protein. The purpose of this experiment was to determine whether a 10 min exposure of FcST2-MMAE to citrate buffers at pH 3.0, 4.0, 5.0 or 6.0 would differently precipitate the HMW forms of this protein. Figure 15 shows that addition of citrate buffer at acidic pH was not successful in precipitating the HMW forms of FcST2-MMAE. The presence of HMW bands was still detected in the gel across all the samples, and the bands had a consistent intensity. However, this experiment demonstrated that the protein could withstand a pH as low as 3.0 without having any impact on the MW distribution as detected by SEC300 analysis. This information is of fundamental importance as it indicates the opportunity to work with this protein across a very wide pH spectrum.

2.3 Stability of FcST2-MMAE in Human Plasma and Serum

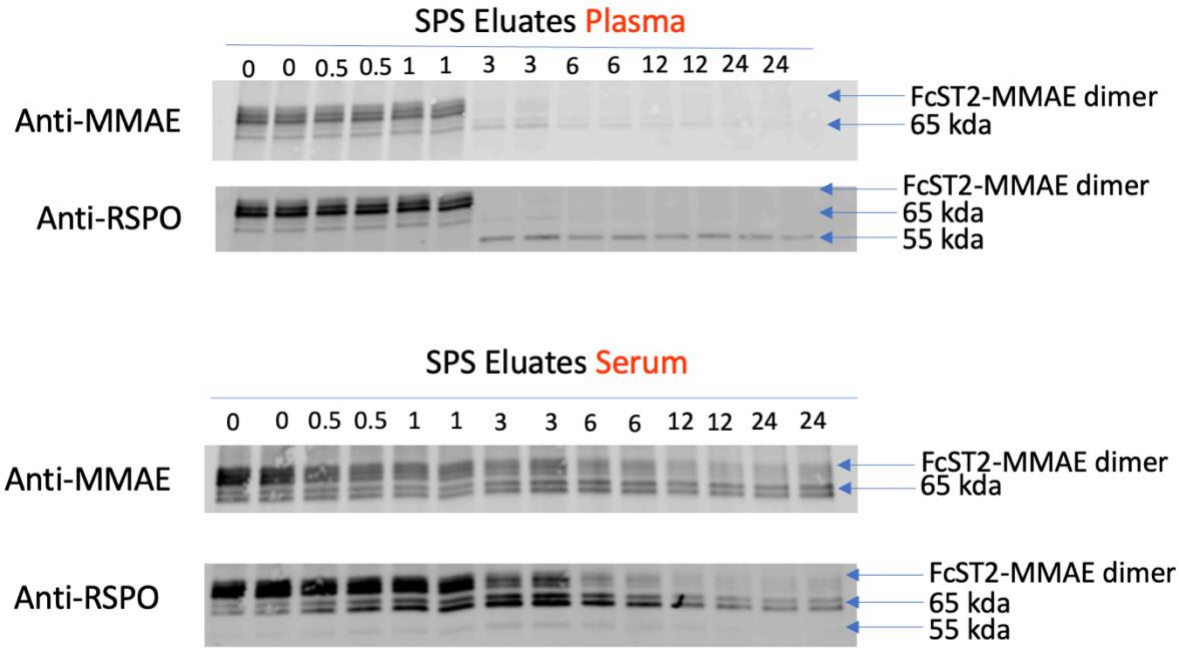

Figure 16. Western Blot Analysis of FcST2-MMAE Samples in Plasma and Serum at Different Time Points.

The FcST2-MMAE sample was added to human plasma and serum samples and incubated for a period of 24 h to explore its stability. Aliquots were collected at different time points as shown in Fig 16 and the protein was captured on an SP resin in order to run a western blot. Each western blot for plasma and serum samples was stained against the anti-MMAE and the anti-RSPO1 domains to analyze the bands observed.

Figure 16 shows that there is a gradual decline of all the bands in serum but in plasma there is a very abrupt decline between 1 and 3 h. Initial degradation rate in plasma and serum is faster for FcF2 dimer than for MMAE dimer. In addition to the dimer band, a pair of bands at about 65 kD was observed in both plasma and serum. A presence of a 55 kD band is observed in plasma

and serum samples but only in the RSPO domains which means this fragment contains the RSPO1 epitope but not the MMAE. This 55 kD band only appears after an hour or more.

2.4 Cytotoxicity of FcST2-MMAE in 8 different ovarian cancer cell lines

A

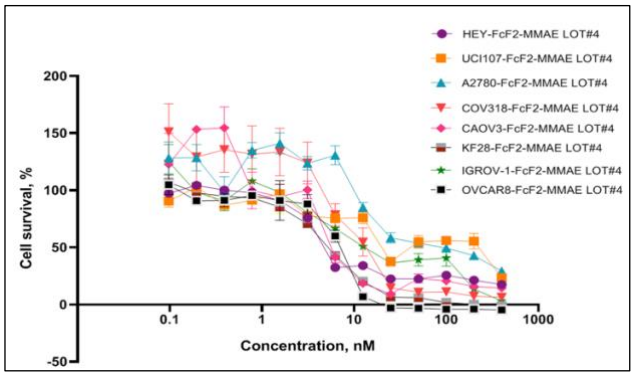

B

Cell line	IC50 nM
HEY	3.83
UCI-107	14.44
A2780	13.44
COV318	7.881
CAOV3	3.101
KF28	5.15
IGROV-1	29.63
OVCAR8	7.35

Figure 17. Analysis of the Potency of FcST2-MMAE Against 8 Human Ovarian Cancer Cell Lines. A. Survival as a function of FcST2-MMAE concentration for 8 human ovarian cancer cell lines. **B.** IC_{50} values for the 8 ovarian cancer cell lines tested.

Among all of the tumor types in the TCGA database, ovarian cancer expresses the among the highest levels of LGR5 and LGR6 mRNA. For this reason, ovarian cancer is a high priority target for the development of FcST2-MMAE. The purpose of this experiment was to determine the potency of this drug across a panel of cell lines representative of this disease. As shown in Figure 17, FcST2-MMAE was remarkably effective at killing these cells with IC_{50} values ranging from 3.8 – 29 nM and all but one cell line having an IC_{50} of less than 20 nM.

DISCUSSION

The rationale for using the receptor binding domain of RSPO1 (R1FF) as a targeting moiety originated from the observation that ovarian cancer expresses high levels of LGR5 and LGR6 mRNA and that LGR5 and LGR6 mark stem cells in the ovarian surface and fallopian epithelia from which ovarian cancers arise. If these receptors are also important to tumor stem cells, then arming R1FF may permit depletion of the stem cell population and slow tumor growth. However, while R1FF-MMAE had good activity this molecule has challenges. To modify this molecule further, a human IgG1 mutant Fc domain was added on to the N terminal end of the molecule to increase stability and half-life of the drug. In addition, the number of LGR binding-domains was increased in order to enhance the overall affinity of the molecule for the LGR5 and LGR6 receptors. With these concepts in mind, the FcST4-MMAE molecule was produced to test the hypothesis.

A functional FcST4-pcDNA3.1 vector was constructed using an overlap PCR strategy. Experiments performed with transient HEK293E cells revealed that the FcST4-His molecule could be produced in mammalian cells and purified using the Ni-NTA and DEAE resin with a yield of 14.3 mg/L culture. HPLC and SDS/PAGE analyses revealed that the FcST4-His protein could be successfully coupled to the MMAE via sortase reaction. More importantly, experiments assessing the stability of FcST4-MMAE at different temperatures and acidic pHs revealed that the molecule, was very stable during storage at 4^{o}C.

However, there were challenges associated with this molecule. The HPLC-C4 and SEC300 traces of FcST4-MMAE revealed that, while the molecule was quite stable during storage at 4oC, it was much less stable if stored at 37^{o}C. The cytotoxicity assays showed that

there was no differential killing observed between the HEK293 cells expressing just an empty vector and cells engineered to over-express LGR5 receptors. The dimeric form of FcST4-MMAE is 120 kD size. This larger size may affect the ability of the FcST4-MMAE molecule to access and bind the LGR receptors. Moreover, the uptake of the molecule into the cell could also have been affected by its larger size. One way to investigate this question further would be to label the molecule with a fluorophore and compare its binding 4^{o}C and its uptake into the interior of the cell at 37^{o}C to that of variants of smaller size.

Another probable issue is that the sticky nature of the ST domains could cause them to fold onto one another leading to intramolecular interactions. These interactions could potentially block the LGR binding domains limit the ability of the molecule to bind to LGR receptors. This issue could be addressed by mutating the 4 ST domains to limit interactions, which will allow all 4 domains to bind LGR receptors.

To test the theory of whether increasing the number of LGR binding domains increased the avidity of the drug, further steps could potentially include using instruments such as the Biacore or the Octet to measure the thermodynamics and binding affinity of the ST-MMAE, FcST2-MMAE and FcST4-MMAE in parallel. Additionally, instrumentation such as Quartz crystal microbalance and FRET can also be used to quantify avidity of the molecule to confirm the hypothesis.

The stability assays for the FcF2-MMAE protein can be further explored by using amino acids or other excipients to stabilize the protein for long term storage. The HPLC and SDS/PAGE analysis revealed that the FcST2-MMAE exists as isomers of multiple molecular weights of some which are high molecular weight aggregates. Ideally these would be removed so as to yield a single dimer band on the gel and a single peak on the HPLC. Additionally, there is a

need to demonstrate selectivity for the FcST2-MMAE drug *in vivo* and define size of the therapeutic window.

In summary, this work demonstrated the feasibility of producing and purifying FcST4-MMAE but also disclosed that additional modifications are required if it is to be advanced into further development.

REFERENCES

Batlle, E., & Clevers, H. (2017). Cancer stem cells revisited. In Nature Medicine (Vol. 23, Issue 10, pp. 1124-1134). Nature Publishing Group. https://doi.org/10.1038/nm.4409

Clarke, M. F. (2019). Clinical and Therapeutic Implications of Cancer Stem Cells. *New England Journal of Medicine*, *380*(23), 2237–2245. https://doi.org/10.1056/nejmra1804280

de Lau, W., Barker, N., Low, T. Y., Koo, B. K., Li, V. S. W., Teunissen, H., Kujala, P., Haegebarth, A., Peters, P. J., van de Wetering, M., Stange, D. E., van Es, J., Guardavaccaro, D., Schasfoort, R. B. M., Mohri, Y., Nishimori, K., Mohammed, S., Heck, A. J. R., & Clevers, H. (2011). Lgr5 homologues associate with Wnt receptors and mediate R-spondin signalling. *Nature*, *476*(7360), 293–297. https://doi.org/10.1038/nature10337

Erlendsson, S., & Teilum, K. (2021). Binding Revisited—Avidity in Cellular Function and Signaling. In *Frontiers in Molecular Biosciences* (Vol. 7). Frontiers Media S.A. https://doi.org/10.3389/fmolb.2020.615565

Ge, Y., Gomez, N. C., Adam, R. C., Nikolova, M., Yang, H., Verma, A., Lu, C. P. J., Polak, L., Yuan, S., Elemento, O., & Fuchs, E. (2017). Stem Cell Lineage Infidelity Drives Wound Repair and Cancer. *Cell*, *169*(4), 636-650.e14. https://doi.org/10.1016/j.cell.2017.03.042

Kim, B., Sun, S., Varner, J. A., Howell, S. B., Ruoslahti, E., & Sailor, M. J. (2019). Securing the Payload, Finding the Cell, and Avoiding the Endosome: Peptide-Targeted, Fusogenic Porous Silicon Nanoparticles for Delivery of siRNA. *Advanced Materials*, *31*(35). https://doi.org/10.1002/adma.201902952

Kopper, O., de Witte, C.J., Lõhmussaar, K. Oded K., Chris J. de Witte Kadi Lõhmussaar, Jose Espejo Valle-Inclan, Nizar H., Lennart K., Anjali Vanita B., Jeroen K., Natalie P., Harry B., Lise M. van W., Sonia Aristín R., Rebecca Theeuwsen, Marieke van de Ven, Markus J. van Roosmalen, Bas P., Victor W. H. Ho, Benjamin G. N., Tjalling B., Katja N. G., Harry V., Maaike P. G. Vreeswijk, Paul J. van Diest, Petronella O. Witteveen, Trudy Jonges, Johannes L. B., Alexander van O., Ronald P. Z., Hugo J. G. S., Wigard P. K. & Hans C. An organoid platform for ovarian cancer captures intra- and interpatient heterogeneity. *Nat Med* 25, 838–849 (2019). https://doi.org/10.1038/s41591-019-0422-6

Lin, P. C., Chan, K. F., Kiess, I. A., Tan, J., Shahreel, W., Wong, S. Y., & Song, Z. (2019a). Attenuated glutamine synthetase as a selection marker in CHO cells to efficiently isolate highly productive stable cells for the production of antibodies and other biologics. *MAbs*, *11*(5), 965–976. https://doi.org/10.1080/19420862.2019.1612690

Lin, P. C., Chan, K. F., Kiess, I. A., Tan, J., Shahreel, W., Wong, S. Y., & Song, Z. (2019b). Attenuated glutamine synthetase as a selection marker in CHO cells to efficiently isolate highly

productive stable cells for the production of antibodies and other biologics. *MAbs*, *11*(5), 965–976. https://doi.org/10.1080/19420862.2019.1612690

Lõhmussaar, K., Kopper, O., Korving, J., Begthel, H., Vreuls, C. P. H., van Es, J. H., & Clevers, H. (2020). Assessing the origin of high-grade serous ovarian cancer using CRISPR-modification of mouse organoids. *Nature Communications*, *11*(1). https://doi.org/10.1038/s41467-020-16432-0

Millstein J, Budden T, Goode EL, Anglesio MS, Talhouk A, Intermaggio MP, Leong HS, Chen S, Elatre W, Gilks B, Nazeran T, Volchek M, Bentley RC, Wang C, Chiu DS, Kommoss S, Leung SCY, Senz J, Lum A, Chow V, Sudderuddin H, Mackenzie R, George J; AOCS Group, Fereday S, Hendley J, Traficante N, Steed H, Koziak JM, Köbel M, McNeish IA, Goranova T, Ennis D, Macintyre G, Silva De Silva D, Ramón Y Cajal T, García-Donas J, Hernando Polo S, Rodriguez GC, Cushing-Haugen KL, Harris HR, Greene CS, Zelaya RA, Behrens S, Fortner RT, Sinn P, Herpel E, Lester J, Lubiński J, Oszurek O, Tołoczko A, Cybulski C, Menkiszak J, Pearce CL, Pike MC, Tseng C, Alsop J, Rhenius V, Song H, Jimenez-Linan M, Piskorz AM, Gentry-Maharaj A, Karpinskyj C, Widschwendter M, Singh N, Kennedy CJ, Sharma R, Harnett PR, Gao B, Johnatty SE, Sayer R, Boros J, Winham SJ, Keeney GL, Kaufmann SH, Larson MC, Luk H, Hernandez BY, Thompson PJ, Wilkens LR, Carney ME, Trabert B, Lissowska J, Brinton L, Sherman ME, Bodelon C, Hinsley S, Lewsley LA, Glasspool R, Banerjee SN, Stronach EA, Haluska P, Ray-Coquard I, Mahner S, Winterhoff B, Slamon D, Levine DA, Kelemen LE, Benitez J, Chang-Claude J, Gronwald J, Wu AH, Menon U, Goodman MT, Schildkraut JM, Wentzensen N, Brown R, Berchuck A, Chenevix-Trench G, deFazio A, Gayther SA, García MJ, Henderson MJ, Rossing MA, Beeghly-Fadiel A, Fasching PA, Orsulic S, Karlan BY, Konecny GE, Huntsman DG, Bowtell DD, Brenton JD, Doherty JA, Pharoah PDP, Ramus SJ. "Prognostic gene expression signature for high-grade serous ovarian cancer." *Annals of oncology: official journal of the European Society for Medical Oncology*vol. 31,9 (2020): 1240-1250. doi:10.1016/j.annonc.2020.05.019

Nathans, J., Hopkins, J., Lebensohn, A. M., & Rohatgi, R. (n.d.). *R-spondins can potentiate WNT signaling without LGRs*. https://doi.org/10.7554/eLife.33126.001

Raslan, A. A., & Yoon, J. K. (2019). R-spondins: Multi-mode WNT signaling regulators in adult stem cells. In *International Journal of Biochemistry and Cell Biology* (Vol. 106, pp. 26–34). Elsevier Ltd. https://doi.org/10.1016/j.biocel.2018.11.005

Schindler, A. J., Watanabe, A., & Howell, S. B. (2018). LGR5 and LGR6 in stem cell biology and ovarian cancer. In *Oncotarget* (Vol. 9, Issue 1). www.impactjournals.com/oncotarget/

Seo, A., Jackson, J. L., Schuster, J. v., & Vardar-Ulu, D. (2013). Using UV-absorbance of intrinsic dithiothreitol (DTT) during RP-HPLC as a measure of experimental redox potential in vitro. *Analytical and Bioanalytical Chemistry*, *405*(19), 6379–6384. https://doi.org/10.1007/s00216-013-7063-2

Testa, U., Petrucci, E., Pasquini, L., Castelli, G., & Pelosi, E. (2018). Ovarian Cancers: Genetic Abnormalities, Tumor Heterogeneity and Progression, Clonal Evolution and Cancer Stem Cells. *Medicines*, *5*(1), 16. https://doi.org/10.3390/medicines5010016

Warden-Rothman, R., Caturegli, I., Popik, V., & Tsourkas, A. (2013). Sortase-tag expressed protein ligation: Combining protein purification and site-specific bioconjugation into a single step. *Analytical Chemistry*, *85*(22), 11090–11097. https://doi.org/10.1021/ac402871k

Witte, M. D., Theile, C. S., Wu, T., Guimaraes, C. P., Blom, A. E. M., & Ploegh, H. L. (2013). Production of unnaturally linked chimeric proteins using a combination of sortase-catalyzed transpeptidation and click chemistry. *Nature Protocols*, *8*(9), 1808–1819. https://doi.org/10.1038/nprot.2013.103

Yu, S., Mulero, M. C., Chen, W., Shang, X., Tian, S., Watanabe, J., Watanabe, A., Vorberg, T., Wong, C., Gately, D., & Howell, S. B. (2021). Therapeutic Targeting of Tumor Cells Rich in LGR Stem Cell Receptors. *Bioconjugate Chemistry*, *32*(2), 376–384. https://doi.org/10.1021/acs.bioconjchem.1c00008

Zhang, S., Dolgalev, I., Zhang, T., Ran, H., Levine, D. A., & Neel, B. G. (2019). Both fallopian tube and ovarian surface epithelium are cells-of-origin for high-grade serous ovarian carcinoma. *Nature Communications*, *10*(1). https://doi.org/10.1038/s41467-019-13116-2

Zhao, Y., Cao, J., Melamed, A., Worley, M., Gockley, A., Jones, D., Nia, H. T., Zhang, Y., Stylianopoulos, T., Kumar, A. S., Mpekris, F., Datta, M., Sun, Y., Wu, L., Gao, X., Yeku, O., del Carmen, M. G., Spriggs, D. R., Jain, R. K., & Xu, L. (2019). Losartan treatment enhances chemotherapy efficacy and reduces ascites in ovarian cancer models by normalizing the tumor stroma. *Proceedings of the National Academy of Sciences of the United States of America*, *116*(6), 2210–2219. https://doi.org/10.1073/pnas.1818357116

Zhao, Y., Yang, S. M., Jin, Y. L., Xiong, G. W., Wang, P., Snijders, A. M., Mao, J. H., Zhang, X. W., & Hang, B. (2019). A Robust Gene Expression Prognostic Signature for Overall Survival in High-Grade Serous Ovarian Cancer. *Journal of Oncology*, *2019*. https://doi.org/10.1155/2019/3614207